AD-A037 047 CONSTRUCTION ENGINEERING RESEARCH LAB (ARMY) CHAMPAI--ETC F/G 11/6
EFFECT OF LACK OF PENETRATION ON FATIGUE RESISTANCE OF HIGH-STR--ETC(U)
FEB 77 Y TOBE, E P COX, F V LAWRENCE

UNCLASSIFIED CERL-TR-M-203 NL

1 OF 1
ADA037047

END

DATE
FILMED
4-77

construction
engineering
research
laboratory

TECHNICAL REPORT M-203
February 1977
Engineering Criteria for Welds

EFFECT OF LACK OF PENETRATION ON FATIGUE RESISTANCE OF HIGH-STRENGTH STRUCTURAL STEEL WELDS

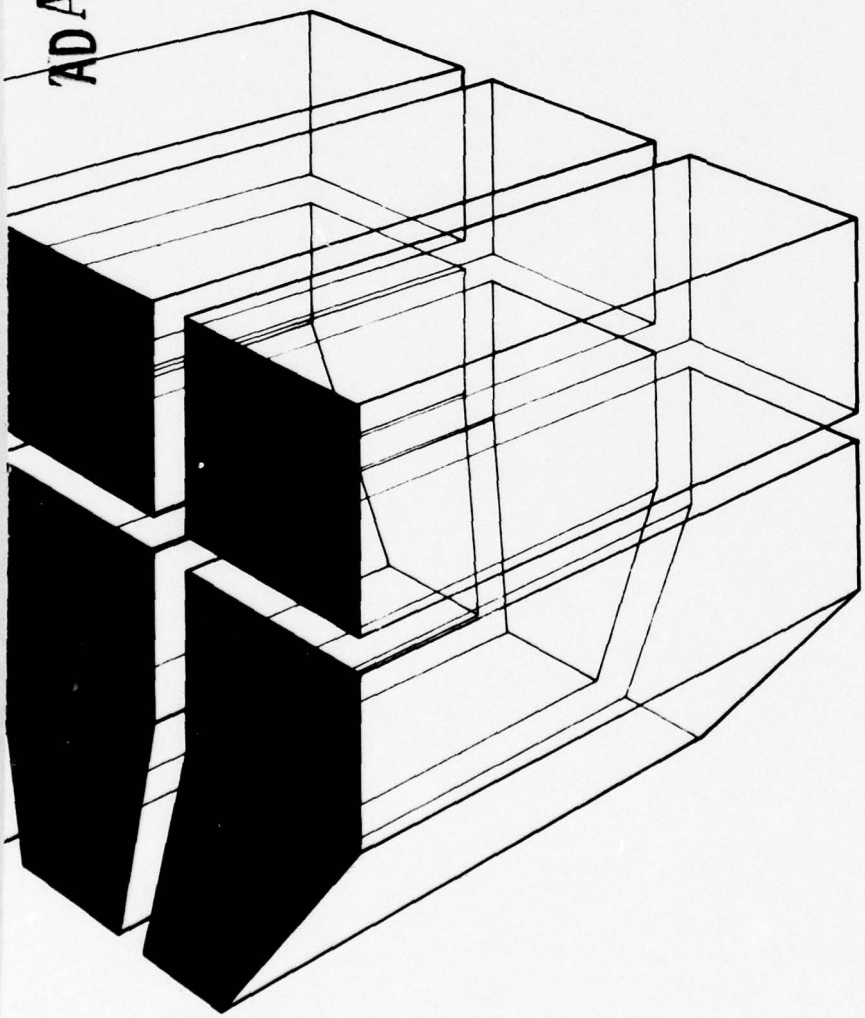

by
Y. Tobe
F. V. Lawrence, Jr.
E. P. Cox

CERL

UNCLASSIFIED

SECURITY CLASSIFICATION OF THIS PAGE *(When Data Entered)*

REPORT DOCUMENTATION PAGE	READ INSTRUCTIONS BEFORE COMPLETING FORM
1. REPORT NUMBER TECHNICAL REPORT M-203 (14) Cerl-TR-M-203	2. GOVT ACCESSION NO. (9) 3. RECIPIENT'S CATALOG NUMBER
4. TITLE *(and Subtitle)* (6) EFFECT OF LACK OF PENETRATION ON FATIGUE RESISTANCE OF HIGH-STRENGTH STRUCTURAL STEEL WELDS	5. TYPE OF REPORT & PERIOD COVERED FINAL rept.,
	6. PERFORMING ORG. REPORT NUMBER
7. AUTHOR(s) (10) Y. Tobe E. P. Cox, F. V. Lawrence, Jr.	8. CONTRACT OR GRANT NUMBER(s)
9. PERFORMING ORGANIZATION NAME AND ADDRESS CONSTRUCTION ENGINEERING RESEARCH LABORATORY P.O. Box 4005 Champaign, Illinois 61820	10. PROGRAM ELEMENT, PROJECT, TASK AREA & WORK UNIT NUMBERS (16) 4DM780120K1[illegible]02-102 (17)
11. CONTROLLING OFFICE NAME AND ADDRESS (12) 30 p.	(11) 12. REPORT DATE Feb[illegible]977 13. NUMBER OF PAGES 28
14. MONITORING AGENCY NAME & ADDRESS *(if different from Controlling Office)*	15. SECURITY CLASS. *(of this report)* UNCLASSIFIED 15a. DECLASSIFICATION/DOWNGRADING SCHEDULE

16. DISTRIBUTION STATEMENT *(of this Report)*

Approved for public release; distribution unlimited.

17. DISTRIBUTION STATEMENT *(of the abstract entered in Block 20, if different from Report)*

18. SUPPLEMENTARY NOTES

Copies are obtainable from National Technical Information Service, Springfield, VA 22151

19. KEY WORDS *(Continue on reverse side if necessary and identify by block number)*

fatigue tests
fatigue resistance
fatigue crack initiation

20. ABSTRACT *(Continue on reverse side if necessary and identify by block number)*

Zero-to-tension fatigue tests were carried out on double-V butt welds of ASTM A514 steel plate, 20 mm in thickness, which contained full-length lack of penetration (LOP) defects. The fatigue crack initiation and propagation portions of the specimens' fatigue lives were experimentally separated. Compression-to-tension fatigue tests were carried out on prime base plate, as-welded sound joints, and reinforcement-removed welds to experimentally determine the fatigue strength reduction factor (K_f) of the LOP defects. → next page

cont.

LOP defects as small as 0.5 mm wide had a profound effect on fatigue life. The fatigue crack initiation life was found to be short—only 10 percent of the total life—and could be predicted using fatigue crack initiation concepts. The use of $K_{f\ max}$, the maximum possible fatigue strength reduction factor, was found to be appropriate.

KF(max)

In a separate substudy, the fatigue resistance of ASTM A514 butt-welded joints containing clustered porosity was determined.

FOREWORD

This research was performed for the Directorate of Military Construction, Office of the Chief of Engineers (OCE) under Project 4DM780120K1, "Engineering Criteria for Design and Construction"; Task 02, "Applications Engineering"; Work Unit 102, "Engineering Criteria for Welds." Mr. I. A. Schwartz was the OCE Technical Monitor.

Drs. Y. Tobe and F. V. Lawrence, Jr. of the Civil Engineering Department of the University of Illinois at Urbana-Champaign conducted the investigation for the Metallurgy Branch (MSM) of the Materials and Science Division (MS), U.S. Army Construction Engineering Research Laboratory (CERL). Their work was done under contract No. DACA 88-75-C-0014.

CERL personnel directly connected with this study were Mr. E. P. Cox, the Principal Investigator.

Dr. G. R. Williamson is Chief of MS and Dr. A. Kumar is Chief of MSM. COL J. E. Hays is the Commander and Director of CERL AND Dr. L. R. Shaffer is Technical Director.

CONTENTS

TABLES

FIGURES

FIGURES (Cont'd)

EFFECT OF LACK OF PENETRATION ON FATIGUE RESISTANCE OF HIGH-STRENGTH STRUCTURAL WELDS

1 INTRODUCTION

Background

The fatigue resistance of welds is usually inferior to that of the metals which they join for at least two reasons. First, the external discontinuities associated with the weld reinforcement or weld bead provide a very severe fatigue notch in butt, fillet, and lap welds. The fatigue resistance of the joint is controlled by the geometry of this notch; unless the notch can be removed or modified by grinding or gas-tungsten-arc (GTA) dressing, for example, the fatigue life of the weldment is essentially fixed for a given loading condition. Second, internal defects such as lack of penetration (LOP), lack of fusion (LOF), weld cracks, and others can provide the critical fatigue notch which has a contributing influence on the fatigue life of the weld. Planar defects such as LOP, LOF, and cracks are particularly serious in this regard.

Because of the severity of the fatigue notch provided by external discontinuities, internal defects are not always the most serious, and generally do not become critical until they become very large or until the weld reinforcement is removed, allowing the internal defect to control fatigue life.

Purpose

The purposes of this study were: (1) to determine the influence of LOP defects on the fatigue life of high-strength steel butt welds, (2) to determine experimentally the fractions of fatigue life devoted to crack initiation and crack propagation, (3) to analytically predict the initiation and propagation portions of life, and (4) to determine the influence of clustered porosity on total fatigue life.

Approach

In this investigation, zero-to-tension (R = O; R being the ratio of the minimum to maximum stress level) fatigue tests were carried out on double-V butt welds of ASTM A514 steel plate, 20 mm in thickness, which contained various width, full-length LOP defects. The initiation and propagation portions of the fatigue life were experimentally separated.

Equal compression-to-tension (R = -1) fatigue tests were carried out on plain plate, as-welded sound joints, and reinforcement-removed welds with several sizes of LOP defects to experimentally determine the fatigue strength reduction factor (K_f) of the toe of the weld and LOP defects.

In a separate study, the fatigue resistance of ASTM A514 butt welded joints containing clustered porosity was determined. The total fatigue life of these specimens is listed in Appendix A.

Mode of Technology Transfer

The information in this report is part of a long-term research effort designed to improve Corps of Engineers guide specifications concerned with the accept/reject levels of weld discontinuities.

2 EXPERIMENTAL PROCEDURES

Materials and Test Specimen Fabrication

Test specimens were made from 20-mm-thick ASTM A514 Grade f steel plates with the chemistry and nominal mechanical properties given in Tables 1 and 2. Table 1 also gives the chemistry of the Murex Hyloy 110 bare wire electrode (1.6 mm diameter) which was used. The mechanical properties of deposited weld metal depend on heat input; the mechanical properties typical for a 1.2 kJ/mm heat input are given in Table 2.

Test specimen blanks were flame-cut from plate stock, keeping the rolling direction parallel to the eventual tensile axis. The blanks were sawed in half, and the edges were prepared with a 60-degree double-V edge having oversize root faces (lands). The halves were welded using one pass per side, 98°C preheat and interpass temperatures, Ar + 2%O_2 shielding gas, a 1.2 kJ/mm heat input, and zero root gap. For land sizes larger than 2 mm, the welding did not completely penetrate the root, resulting in the creation of full-length LOP defects ranging from 1 to 8 mm in width ($2a_o$), which were oriented perpendicular to the tensile axis (Figure 1). The welded test specimens were machined to the dimensions shown in Figure 2. Figure 3 shows a typical weld profile. The test specimens were fatigue-tested with the reinforcement intact, except for a few compression-to-tension (R = -1) tests for which it was removed by surface grinding. The test specimens were x-ray radiographed prior to

testing to insure that they were suitable for testing and included the desired LOP.

In addition to the specimens containing full-length LOP defects described above, sound weld (containing no LOP) and prime base plate test pieces of similar dimensions were prepared. The following code was used to identify the various types of test pieces:

- P = prime base plate with mill scale intact
- W = sound welds with weld reinforcement intact
- LN = test pieces with weld reinforcement intact and full-length LOP defects
- LF = reinforcement-removed test pieces containing full-length LOP defects.

Fatigue Testing

All fatigue tests were performed under load control using a closed-loop hydraulic test system. Specimens were mounted in the test frame and gripped with self-aligning grips. Testing was carried out under ambient laboratory conditions at a rate of 1 to 15 Hz. The load cycle was zero-to-tension (R = 0) for the W and LN test pieces and compression-to-tension (R = -1) for the long-life W and LF tests.

Strains near the LOP of some LN test pieces were monitored by strain gages (Micro Measurements EA-06-031CF-120) mounted 2 mm from the tip of the LOP defect (Figure 3). The peak dynamic strains were monitored during the test. Changes in these readings indicated a small enlargement of the original LOP defects. The significance of these strain changes in terms of crack advance was determined by heat-tinting and ink-stain methods. The initial size of the LOP defect was measured on the fracture surface after completion of the test. Strain gage measurements were not made on the other specimens since only the life to failure was the measured variable.

3 RESULTS

Fatigue Data

Tables 3, 4, and 5 give the results of all the fatigue tests. Table 3 gives the results for sound welds (R = 0) (W series). Table 4 gives the results of (R = 0) tests on welds with reinforcement intact containing full-length LOP defects (LN series), and Table 5 gives results for long-life (R = -1) tests run to determine the fatigue strength reduction factor (K_f).

The S-N diagram shown in Figure 4 compares the results of the sound weld (W series) tests with data from the literature.[1] The test results lie within the 99 percent confidence limits for A514 butt welds and are thus typical for such welds. Figure 5 shows the test data for the welds containing LOP defects (LN series); the data confirm the serious effect that such defects may have on fatigue resistance. The size of the LOP influenced life greatly, with the effect ranging from a slight reduction in life to as much as an order of magnitude reduction. Figure 6 shows the results of compression-to-tension fatigue tests (R = -1) on prime base plate, sound welds, and welds containing LOP defects.

Fatigue Crack Initiation and Propagation Locations

Figures 7 and 8 are macrographs of the fatigue crack initiation and propagation locations in the sound (W series) and LOP-containing (LN series) test pieces. Figure 7 shows several toe initiation sites typical of the sound welds and welds containing very small LOP defects. It is interesting to note that initiation and early crack growth often occurred in the weld metal. Figure 8 shows the influence of LOP size on the initiation sites and propagation paths for welds containing full-length LOP defects (LN series). At the largest LOP widths (Figure 8d) the LOP clearly dominates; in all cases, however, there is some interaction between the toe and the LOP defect. At the smaller LOP widths (Figures 8a and b), initiation and propagation at the weld toe dominate. Although the initiation and propagation patterns are complex, it should be remembered that the final stages of fracture, during which these complex patterns develop, occur only during the very last stages of the fatigue life.

Detecting Crack Initiation and Early Growth

Figure 9 shows the typical peak strain histories measured by strain gages located approximately 2 mm from the tip of an LOP defect in specimen LN-37. The peak strain remains relatively constant during the early portions of the fatigue life but begins to increase after about 1000 cycles. At 4000 cycles, the specimen was removed from the test frame and cut in half lengthwise. One half was ink-stained and the other heat-tinted to determine the crack advance associated with the 85 x 10^{-6} peak strain increase. The specimen halves were then fractured in monotonic tension. Examination of the fracture surfaces revealed a 0.78-mm increase in LOP width (0.39 mm increase in the half-width). Heat-tinting and ink-staining methods gave the same result.

[1] W. H. Munse, et al., *Fatigue Data Bank and Data Analysis Investigation*, Structural Research Series No. 405 (University of Illinois at Urbana-Champaign, June 1973).

The increased strain reading is related either to the stresses associated with the tip of the advancing crack or to increases in the net section stress or both. An analysis of the state of stress in the vicinity of the strain gages revealed that, at the location 2 mm from the crack tip, the stress is approximately equal to the net section stress. Using the simplest approximation:

$$\Delta\epsilon \approx \frac{P}{EW}\left[\frac{1}{t-(2a_0+2\Delta a)} - \frac{1}{t-2a_0}\right] \quad \text{[Eq 1]}$$

where:

$\Delta\epsilon$ = strain increase due to a crack advance $2\Delta a$

$2\Delta a$ = crack advance

$2a_o$ = initial LOP width

t = weld thickness $\approx$ plate thickness

W = test piece width

E = Young's modulus

P = load on test piece.

It was determined that if $2a_o$ equalled 4.8 mm, for example, a crack advance ($2\Delta a$) of 0.254 mm would produce a strain change $\Delta\epsilon$ of 22×10^{-6}. To further test this prediction, specimen LN-36 was fatigued close to the predicted strain change (Figure 10). The measured crack advance ($2\Delta a$) was 0.20 mm as compared with the 0.254 mm predicted. In any case, a change of peak dynamic strain of 19×10^{-6} represents a very small (~0.1 mm) increase in LOP half-width or approximately 0.2 mm in full width.

The measured crack initiation life (N_I), determined assuming a crack advance (Δa) of 0.127 mm as the division between initiation (and early crack growth) and fatigue crack propagation, is tabulated in Table 6 and plotted versus LOP defect width in Figure 11. The measured initiation life (N_I) is relatively short (approximately 10 percent of the total life) and depends strongly on LOP defect width and the applied stress level. The percentage of life devoted to initiation is plotted as a function of total life (N_T) in Figure 12.

4 DISCUSSION

Fatigue Crack Initiation Life at LOP Defects

As seen in Table 6 and Figure 12, the fatigue crack initiation life (N_I) is quite short compared to the total fatigue life. This result is not too surprising, since the LOP defects are flat, cracklike defects oriented in the worst possible attitude, i.e., perpendicular to the fluctuating tensile stress.

To estimate the fatigue crack initiation life (N_I) using low-cycle fatigue concepts, several simplifying assumptions were made: the mean stress for all tests was assumed to decay to zero after very few cycles so that at the tip of the LOP, the mean stress is taken to be zero. Second, it was assumed that the elastic strains at the LOP tip are small relative to the plastic strains; this assumption should be valid if both the measured and calculated initiation lives are less than the transition fatigue life (N_{tr}) of the material, at which the elastic and plastic cyclic strains are equal by definition. Third, it was assumed that a modified Neuber relation estimates the product of stress and strain ($\sigma \cdot \epsilon$) at the tip of the LOP defect:[2]

$$\frac{(SK_f)^2}{E} = \sigma \cdot \epsilon \quad \text{[Eq 2]}$$

where:

S = remotely applied stress

K_f = fatigue notch factor = $\dfrac{\text{fatigue strength without stress concentration}}{\text{fatigue strength with stress concentration}}$

E = Young's modulus

σ = notch tip stress range

ϵ = notch tip strain range.

The first difficulty is estimating K_f. Peterson's equation[3] gives a relationship between K_f and the elastic stress concentration factor (K_t) and requires knowledge of a microstructural parameter (A) and the notch root radius (r):

$$K_f = 1 + \frac{K_t - 1}{1 + \frac{A}{r}} \quad \text{[Eq 3]}$$

[2] R. J. Mattos, *Estimation of the Fatigue Crack Initiation Life in Welds Using Low Cycle Fatigue Concept*, Ph.D. Thesis (University of Illinois at Urbana-Champaign, 1975); and H. Neuber, "Theory of Stress Concentration for Shear Strained Prismatical Bodies with Arbitrary Non-Linear Stress-Strain Laws," *Journal of Applied Mechanics* (December 1961), p. 544.

[3] R. E. Peterson, "Fatigue of Metals III—Engineering and Design Aspects," *Materials Research and Standards*, Vol 6, No. 6 (February 1963), p. 313.

and for an elliptical flaw:

$$K_t = 1 + 2\left(\frac{a}{r}\right)^{1/2} \qquad \text{[Eq 4]}$$

where:

a = LOP half width

r = LOP tip radius.

Peterson's equation becomes:

$$K_f = 1 + \frac{2\left(\frac{a}{r}\right)^{1/2}}{1 + \frac{A}{r}} \qquad \text{[Eq 5]}$$

Values of K_f predicted by this equation achieve a maximum value ($K_{f\ max}$) for values of r equal to A.

$$K_{f\ max} = 1 + \left(\frac{a}{A}\right)^{1/2} \qquad \text{[Eq 6]}$$

This maximum value of K_f is assumed to occur at some location at the tip of the LOP, which constitutes the most severe location.

Values of A in Peterson's equation for steels are given in the literature and also by the relationship[4]

$$A \cong 3.937 \times 10^{-5} \left(\frac{2068}{S_u}\right)^{1.8} \text{ (S.I. units)} \qquad \text{[Eq 7]}$$

Figure 13 compares K_f values calculated using $K_{f\ max}$ (Eq 6) and experimental long-life (failure greater than 10^6 cycles) fatigue test results. The K_f values calculated from R = -1 tests (Table 5 and Figure 6) lie below the calculated $K_{f\ max}$ values, but it must be remembered that the total life of these tests includes an unknown amount of propagation. The LN series tests (Table 6) in which N_I was measured provide a second comparison. Using N_T for prime base plate and N_I from the R = 0 tests (Figure 14) gives a much higher calculated value of K_f, presumably because the N_T for the prime base plate also include some propagation. Probably the best experimental values are provided by the R = -1 tests; as is seen in Figure 13, the agreement between $K_{f\ max}$ and these data is closest.

To develop an expression estimating the cycles to crack initiation (N_I) Eq 2 is rewritten as follows:

$$(SK_{f\ max})^2 = 4E \cdot \sigma_a \cdot \frac{\Delta\epsilon}{2} \qquad \text{[Eq 8]}$$

[4] R. E. Peterson.

where

σ_a = stress amplitude = $\frac{\Delta\sigma}{2}$

$\frac{\Delta\epsilon}{2}$ = total strain amplitude

Now

$$\frac{\Delta\epsilon}{2} \approx \frac{\Delta\epsilon_p}{2} = \epsilon_f'(2N_I)^c \qquad \text{[Eq 9]}$$

for lives less than N_{tr}. It is also true that:

$$\sigma_a = \sigma_f'(2N_I)^b \qquad \text{[Eq 10]}$$

where:

$\frac{\epsilon_p}{2}$ = plastic strain amplitude

ϵ_f' = fatigue ductility coefficient

c = fatigue ductility exponent

σ_f' = fatigue strength coefficient

b = fatigue strength exponent

N_I = crack initiation life.

Combining Eqs 8, 9, and 10

$$(SK_f)^2 = 4\,E\,\sigma_f'\,\epsilon_f'\,[2N_I]^{b+c} \qquad \text{[Eq 11]}$$

or, using Eq 6 for $K_{f\ max}$ and recalling that $\Delta K_o \cong S\sqrt{\pi a_o}$,

$$N_I \cong \frac{1}{2}\left[\frac{\sqrt{4\pi\,A\,E\,\sigma_f'\,\epsilon_f'}}{\Delta K_o}\right]^{\frac{2}{|b| + |c|}} \qquad \text{[Eq 12]}$$

A more detailed derivation of Eq 12 is given in Appendix B. Values of N_I predicted by Eq 12 and strain-controlled fatigue data for one-pass E110 weld metal (Table 7) are plotted as a dashed line in Figure 15. As predicted by Eq 12, the relationship between N_I and ΔK_o is a power law. The slope of the experimental data is -3 and the slope predicted by Eq 12 (i.e., $\frac{2}{|b| + |c|}$) is -2.97. The agreement between experiment and calculation is better than would be expected. Although this agreement may be fortuitous, several conclusions can be drawn: the mean stress must relax at the tip of the LOP defect, the strains at the tip of the LOP defect are predominantly plastic, and the use of $K_{f\ max}$ is apparently appropriate.

Fatigue Crack Propagation Life

The major portion of life of the specimens containing LOP defects was devoted to fatigue crack propagation. The initiation life, while finite and predicted by low-cycle fatigue concepts, was seen to be so short for the stresses and strains investigated that there is little difference between the total fatigue life (N_T) and the fatigue crack propagation portion of total life (N_P). Table 6 lists the total, initiation, and propagation lives, and Figure 16 plots the total fatigue life against LOP defect width ($2a_o$). The solid lines in this figure have been calculated using the power law relationship for fatigue crack growth,[5]

$$\frac{da}{dN} = C(\Delta K)^n \qquad \text{[Eq 13]}$$

and the stress intensity factor for a center-cracked plate having finite dimensions is defined by:

$$\Delta K = S\sqrt{\pi a}\left\{\sec\frac{\pi a}{t}\right\}^{1/2} \qquad \text{[Eq 14]}$$

This leads to an expression which predicts N_P as a function of stress range (S) and initial and final LOP defect half-width (a_o, a_f):

$$N_P = \frac{1}{C}\int_{a_0}^{a_f}\left\{S\sqrt{\pi a}\left(\sec\frac{\pi a}{t}\right)^{1/2}\right\}^{-n} da \qquad \text{[Eq 15]}$$

where t is the plate thickness, and the values of C and n (the materials properties in Eqs 13 and 15) which best fit the experimental data were found to be:

$$n = 3.32$$
$$C = 4.68 \times 10^{-9}\ (\text{MPa}\sqrt{\text{m}})$$

These values are similar to those reported by Bucci et al[6] for T-1 steel (base metal).

Influence of LOP on Fatigue Life

Cracklike defects such as LOP are serious defects which greatly reduce the fatigue life of welds in which they exist. As seen in Figures 5, 11, 15, and 16, the influence of full-length LOP defects upon life is a very strong function of the width of the defect ($2a_o$). A major reason for the short lives produced by these defects is that the initiation portion of life is reduced to insignificant values due to the high stress concentration at the tip of the defect. Consequently, for specimens loaded above the threshold value of K (ΔK_{th}), the majority of life is spent in propagation.

Even the smallest defect studied –0.5 mm wide, 6 mm long (a less than full-length LOP, specimen LN-20)– resulted in a life shorter than the average for sound butt welds with reinforcement intact. If the fatigue resistance of sound butt welds is viewed from a statistical standpoint and the lower confidence limit for sound weld data is used as a criterion, then, as seen in Figure 5, LOP defects with widths ($2a_o$) slightly larger than 1 mm would be tolerable, because they would produce lives no shorter than the lower confidence limit for sound butt welds (Figure 16).

5 SUMMARY AND CONCLUSIONS

Flat, cracklike defects such as LOP have a profound effect on the fatigue resistance of butt welds (Figures 3, 4, and 5). Results of this study showed that LOP defects as small as 0.5 mm wide reduced the fatigue life below the normal expectancy for sound welds; however, LOP defects as large as 1 mm may be tolerated if the lower confidence limit for sound weld data is adopted as a criterion (Figure 16).

The initiation life of LOP defects, as defined and measured, was shown to be very short (less than 10 percent of total life) and could be predicted using fatigue crack initiation concepts and low-cycle fatigue data for E110 weld metal. The agreement between the measured and predicted initiation lives suggests that the mean stresses at the tip of the LOP defect decay rapidly and that the fatigue strength reduction factor (K_f) associated with the LOP is very close to the maximum possible K_f calculated using Peterson's equation (Eq 6).

The fatigue crack propagation portion of life was explained in terms of the power law for fatigue crack growth and was seen to occupy over 90 percent of the total life in the life range 10^3 to 10^6 cycles.

---

[5] P. C. Paris et al., "A Critical Analysis of Crack Propagation Laws," *Trans. ASME (D)*, Vol 85, No. 4 (1963).

[6] R. J. Bucci et al., *Fatigue Crack Propagation Growth Rates Under a Wide Variation of ΔK for an ASTM A-517 Grade F (7 - 1) Steel*, ASTM STP 513 (American Society for Testing and Materials, September 1972).

Table 1

Chemical Composition of Base Metal (A514-F Plate) and Welding Electrode (1.6 mm Diameter Bare Wire)* (wt %)

Element	C	Si	Mn	P	S	Cu	Ni	Cr	Mo	V	B	Ti	A2
Base Metal**	.16	.23	.82	.012	.019	.27	.76	.54	.47	.06	.004	--	--
Welding Electrode	.08	.46	1.70	.005	.009	--	2.40	.05	.50	.02	--	.025	.003

* Compositions supplied by manufacturer.
** Ladle composition.

Table 2

Small Specimen Tensile Properties for Base Metal and Weld Metal

Material		Yield Strength S_y (MPa)	Ultimate Strength S_u (MPa)
Base Metal*	Longitudinal	762.9	842.3
	Transverse	730.5	846.2
Weld Metal**		871.7	966.9

* Overall specimen length 102 mm, 25.4 mm gage length, 5.66 mm diameter reduced section.
** Overall specimen length 127 mm, 25.4 mm gage length, 7.98 mm diameter reduced section. Heat input 1.2 kJ/mm.

Table 3

Results of (R = 0) Fatigue Tests on Sound Welds With Reinforcement Intact

Specimen	Gross Stress (MPa)	Total Fatigue Life (Cycles)	Fracture mode: Crack Initiation Site	Fracture mode: Crack Propagation Path
W-5	412	215,000	toe (in WM)	WM → HAZ
W-7	412	159,000	toe (in WM)	Bond → HAZ
W-8	206	4,930,000	none	none
W-9	412	110,000	toe	HAZ
W-10	275	1,050,000	none	none
W-10*	309	1,030,000	toe	HAZ
W-12	240	4,950,000	none	none
W-12*	275	730,000	toe	HAZ
W-13	275	319,000	toe (in WM)	WM → HAZ

*Retested at higher stress level

Table 4

Results of (R = 0) Fatigue Tests on As-Welded Test Pieces Containing Full-Length LOP Defects

Specimen	Width at LOP $2a_o$ (mm)	Gross Stress Range (MPa)	Total Fatigue Life (Cycles)	Fracture mode: Crack Initiation Site	Fracture mode: Crack Propagation Path
LN-14	2.01	412	13,100	LOP	WM
LN-15	1.78	206	252,000	LOP	WM
LN-16	1.21	206	256,000	LOP (+ toe)	WM (LOP)
LN-17	1.68	206	184,000	LOP	WM
LN-18	1.88	206	166,000	LOP	WM
LN-19	0.89	412	28,200	LOP (+ toe)	HAZ (toe)
LN-20	0.50*	412	57,300	LOP (+ toe)**	HAZ
LN-22	7.00	206	70,600	LOP	WM
LN-23	6.40	412	4,070	LOP	WM
LN-24	6.67	206	82,900	LOP (+ toe)	WM (LOP)
LN-25	5.31	206	58,400	LOP (+ toe)	WM (LOP)
LN-26	7.09	412	3,190	LOP	WM
LN-27	7.28	412	3,370	LOP	WM
LN-28	7.51	206	49,000	LOP	WM
LN-29	6.76	206	38,300	LOP (+ toe)	WM (LOP)
LN-31	4.06	412	5,960	LOP	WM
LN-34	5.03	206	64,100	LOP (+ toe)	WM (LOP)
LN-35	4.75	412	6,210	LOP	WM
LN-43	2.47	206	143,000	LOP	WM
LN-45	1.41	412	22,100	LOP (+ toe)	WM (LOP)

* Length of the LOP, 6 mm.
** Crack initiated from two different toes, separately.

Table 5

Results of (R = -1) Fatigue Tests on ASTM A514 Prime Base Plates, Sound Welds and LOP Specimens

Specimen	Gross Stress Range (MPa)	Total Fatigue Life (Cycles)	Fracture mode: Crack Initiation Site*	Fracture mode: Crack Propagation Path
P-2	412	5,000,000+	no sign of crack	
P-2**	480	5,000,000+	no sign of crack	
P-3	824	185,000	reduced section	
P-4	618	379,000	reduced section	
W-40	412	613,000	toe	HAZ
W-41	549	190,000	toes	HAZ
W-42	686	265,000	toe	HAZ
W-43	490	935,000	toe	HAZ
LF-30	127	889,000	LOP (2.68)	WM
LF-32	275	121,000	LOP (5.62)	WM
LF-33	176	547,000	LOP (2.95)	WM

* Numbers in parentheses indicate the average width of the full-length LOP defects.
** Retested at higher stress level.
\+ Run out.

Table 6

Measured Fatigue Crack Initiation and Fatigue Crack Propagation Lives

Specimen	Gross Stress Range R = 0 (MPa)	Defect Width $2a_o$ (mm)	N_T Cycles	N_I* (measured) Cycles	N_p (measured) Cycles
LN-17	206	1.68	184,000	12,500	171,500
LN-18	206	1.88	166,000	11,800	154,200
LN-22	206	7.00	70,600	1,850	68,750
LN-26	412	7.09	3,190	145	3,045
LN-27	412	7.28	3,370	135	3,235
LN-28	206	7.51	49,000	2,750	46,250
LN-29	206	6.76	38,300	2,050	36,750
LN-31	412	4.06	5,960	300	5,660
LN-34	206	5.03	64,100	3,750	60,350
LN-36	206	4.80	--	2,100	--
LN-37	206	6.30	--	1,600	--
LN-43	206	2.47	143,000	5,800	137,200
LN-45	412	1.41	22,100	2,450	19,650
LN-47	137	2.50	--	155,000	--

* Crack initiation based on a detectable crack advance of 0.127 mm.

Table 7

Low-Cycle Fatigue Properties*

E	= 207,887 MPa	c	= -0.590
σ'_y	= 600 MPa	n'	= 0.128
σ'_f	= 1359 MPa	σ_f	= 1406 MPa
ϵ'_f	= 0.595	$2N_{tr}$	= 6944 reversals
b	= -0.0785		

* Data obtained as part of this study.

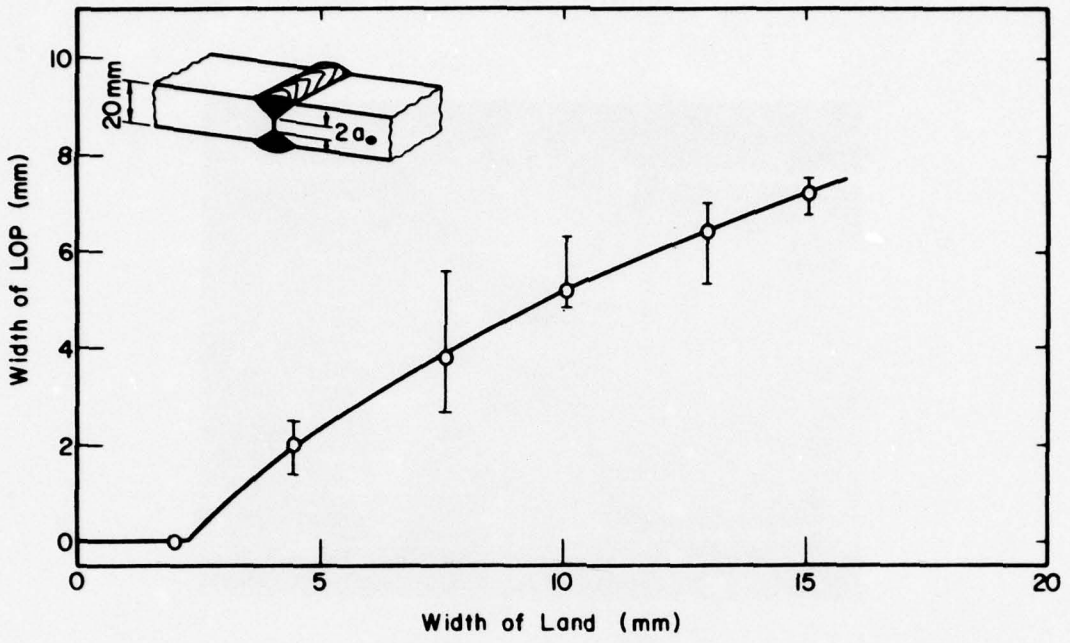

Figure 1. Relationship between the width of edge land and the width of the LOP defect obtained after welding.

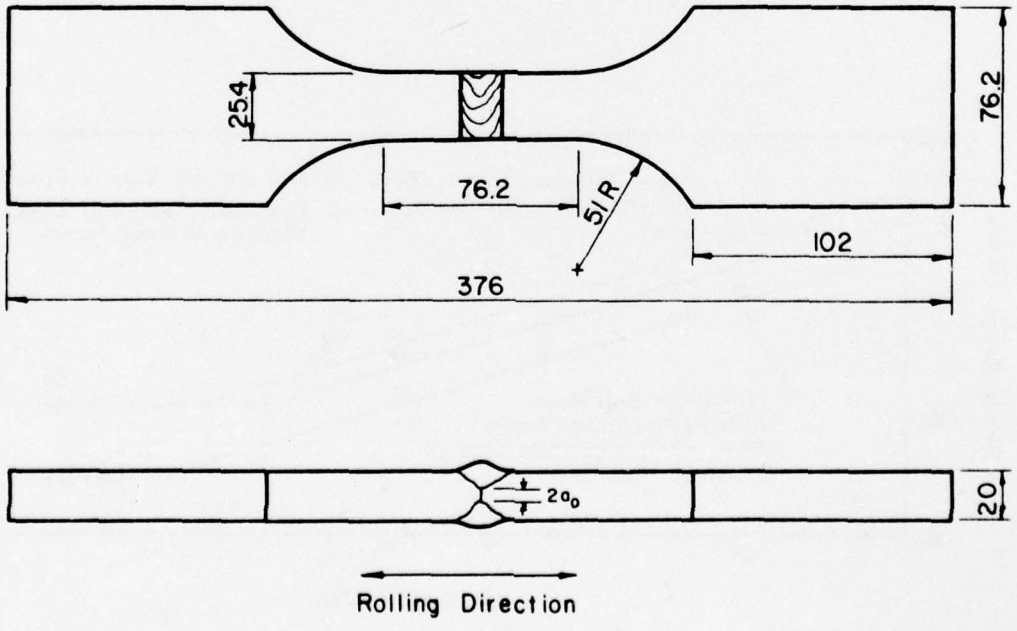

Figure 2. Machined dimensions of test specimens. All dimensions in millimeters.

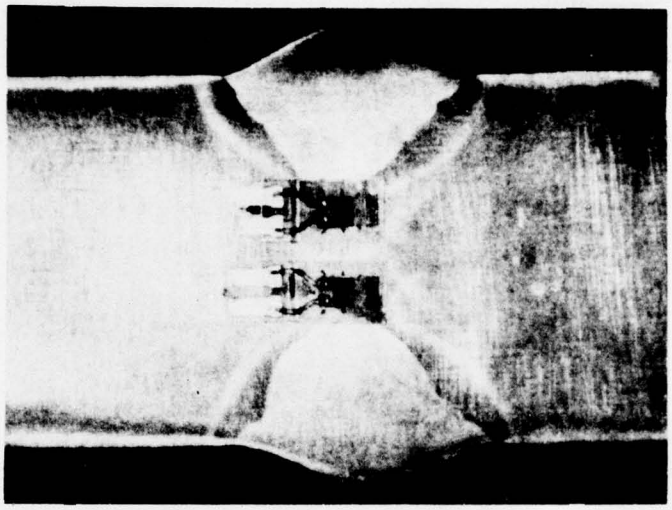

Figure 3. Macrograph profile of weld containing an LOP discontinuity. Strain gages are located approximately 2 mm from tips of LOP.

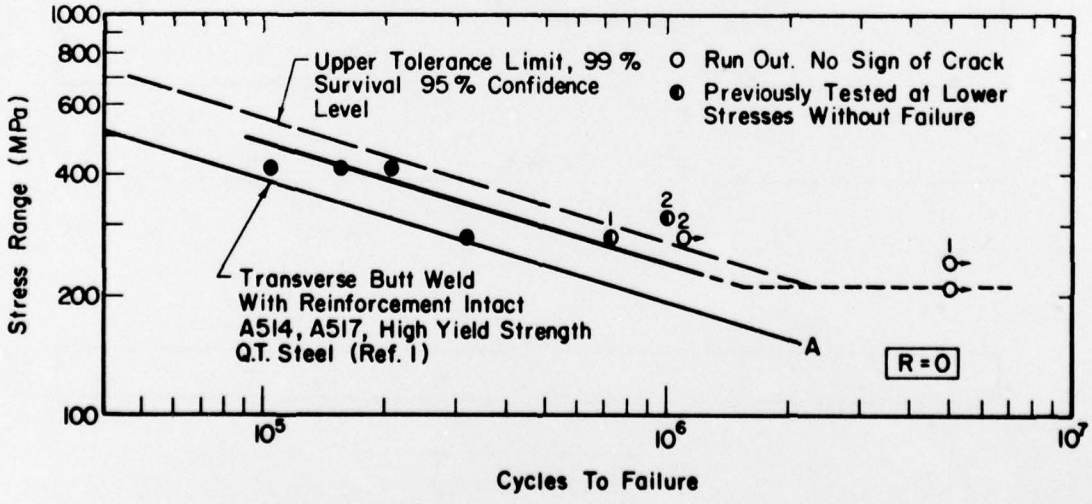

Figure 4. S-N curve for sound welds (W series).

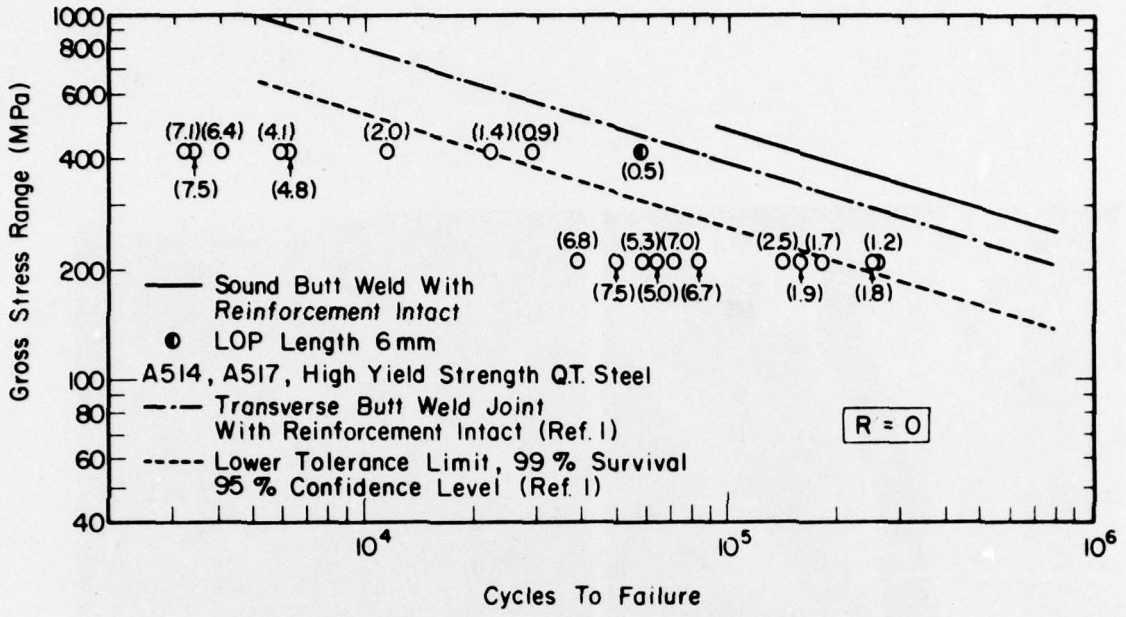

Figure 5. Fatigue test results for butt welds containing full-length LOP defects. The average LOP widths in millimeters ($2a_0$) are indicated in parentheses.

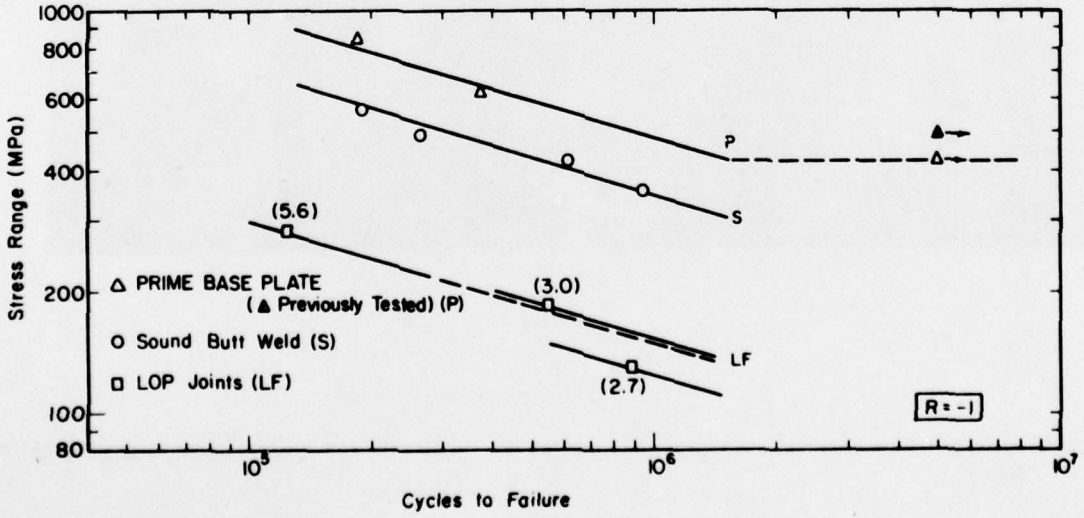

Figure 6. Compression-to-tension fatigue data for prime base plate, sound welds, and LOP-containing welds. The LOP widths in millimeters ($2a_0$) are shown in parentheses.

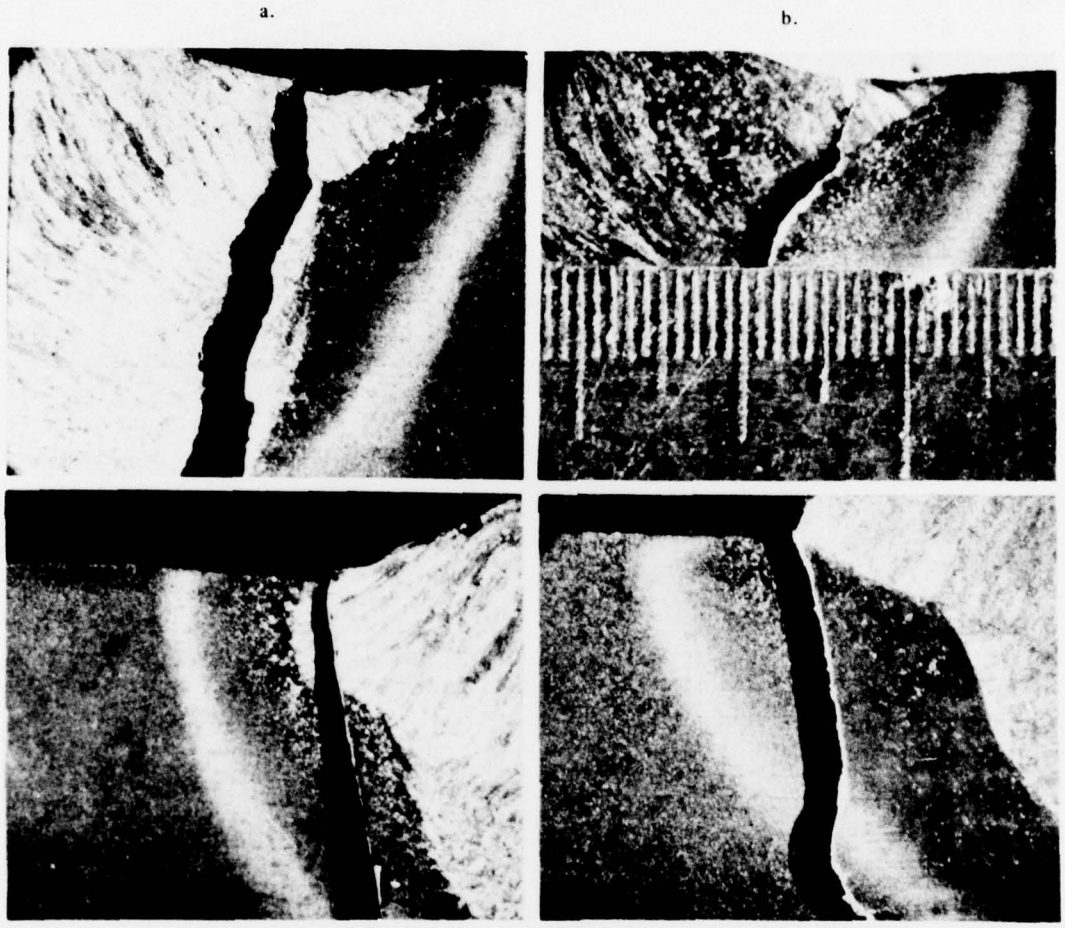

Figure 7. Crack initiation sites and crack propagation paths for sound welds. (R = 0) (Gradations on scale in b are 0.01 in.)

a. W-5	N_T = 215,000	S = 412 MPa
b. W-7	N_T = 159,000	S = 412 MPa
c. W-13	N_T = 319,000	S = 275 MPa
d. LN-19	N_T = 28,200	S = 412 MPa

a. b.

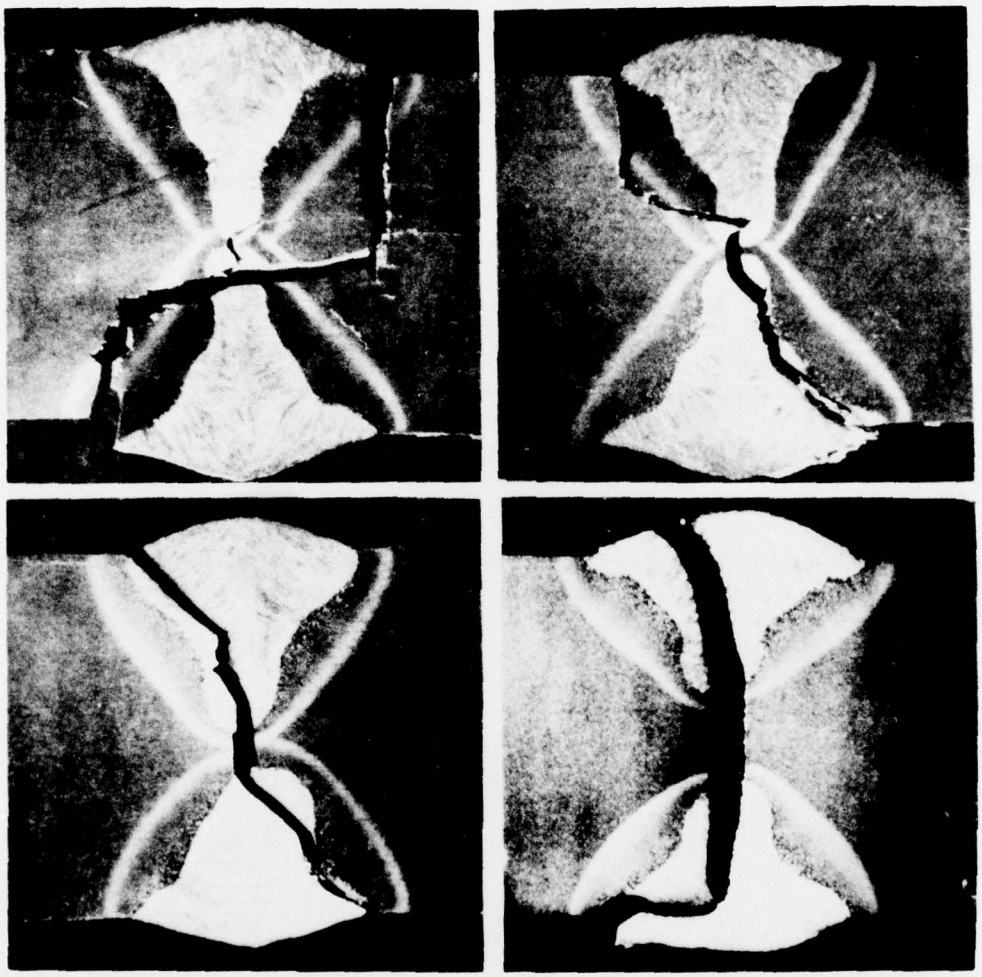

c. d.

Figure 8. Crack initiation sites and crack propagation paths for welds containing LOP defects. (R = 0) (magnification $\simeq$ 2.7x)

a. LN-20 (0.5, 6)	N_T = 57,300	S = 412 MPa
b. LN-19 (0.9, full)	N_T = 28,200	S = 412 MPa
c. LN-14 (2.0, full)	N_T = 13,100	S = 412 MPa
d. LN-25 (5.3, full)	N_T = 58,300	S = 206 MPa

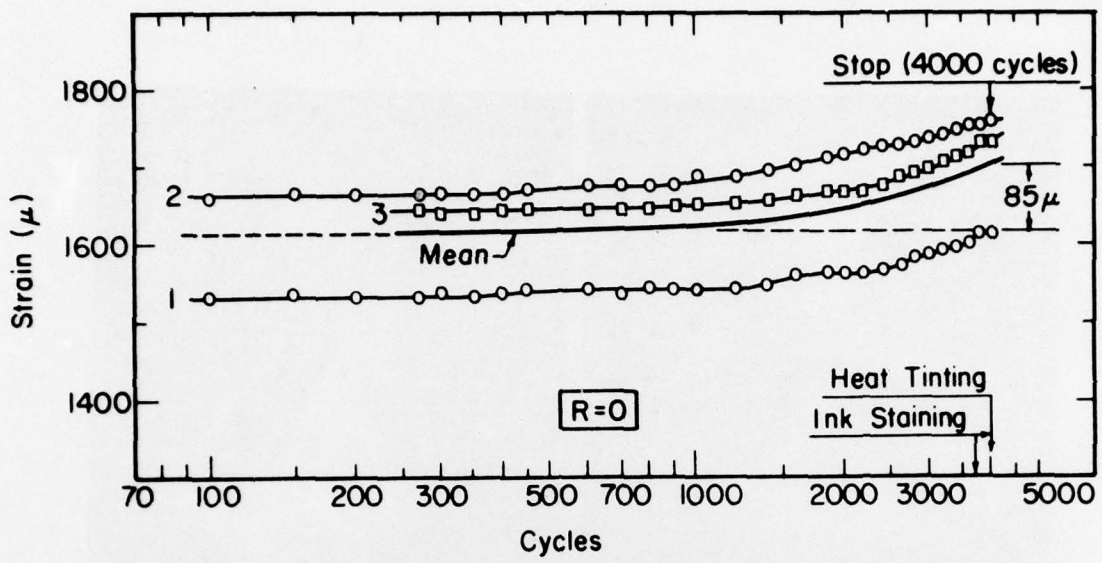

Figure 9. Peak dynamic strain near the tips of LOP in specimen LN-37 which was tested under a stress range of 206 MPa and contained a 6.3 mm width LOP. The strain change of 85 x 10^{-6} corresponded to a half-width increase of 0.39 mm.

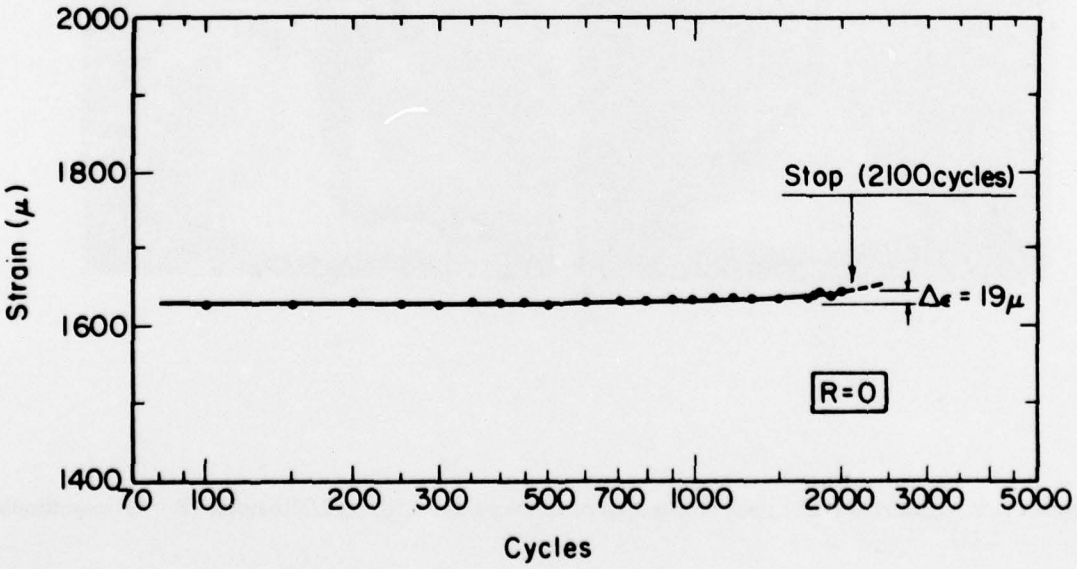

Figure 10. Peak dynamic strain near tip of LOP in Specimen LN-36 which was tested under a stress range of 206 MPa and which contained a 4.8 mm width LOP. The strain change of 19 x 10^{-6} corresponded to a half-width increase of 0.1 mm.

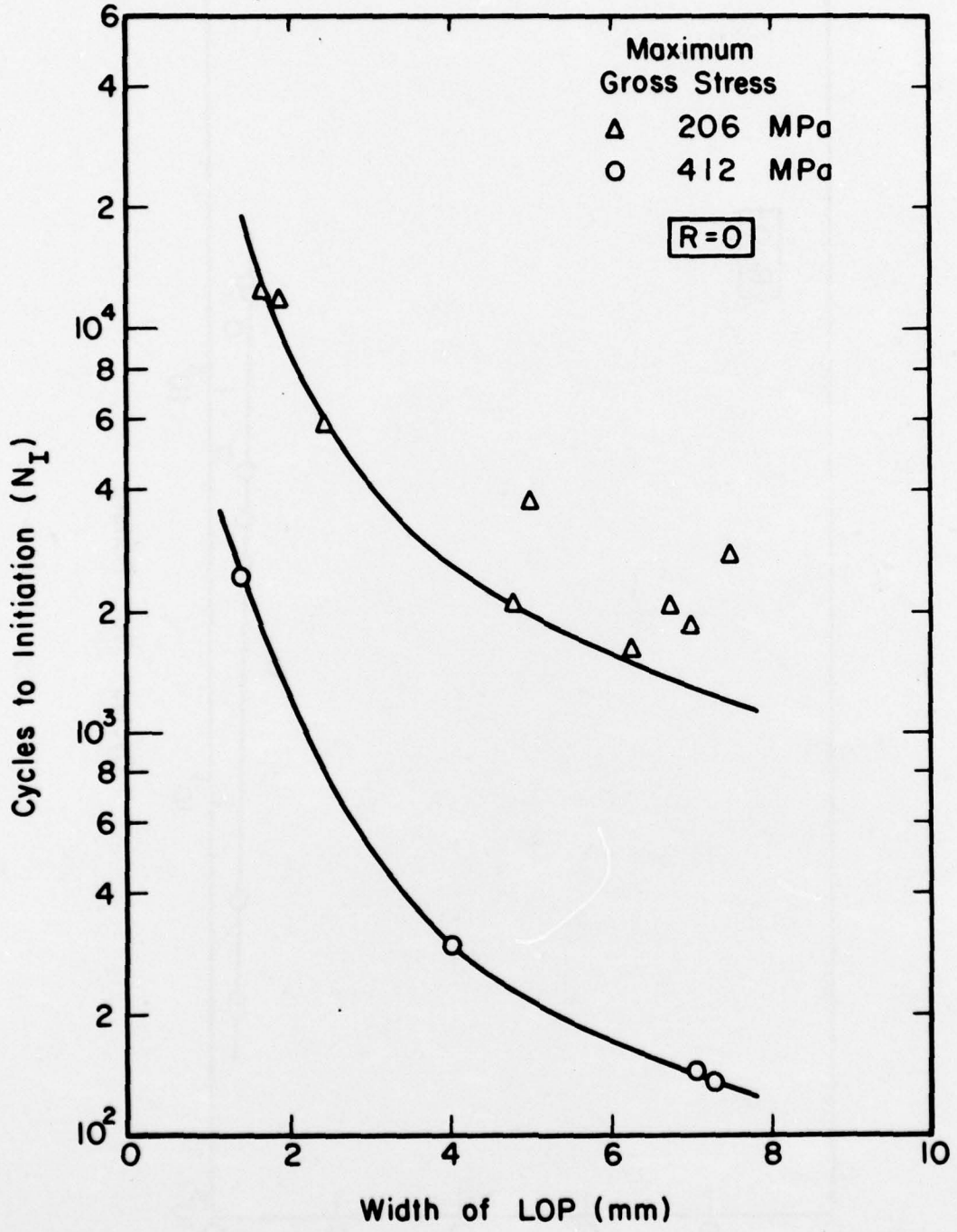

Figure 11. Relationship between LOP width ($2a_o$) and measured fatigue crack initiation life (N_I).

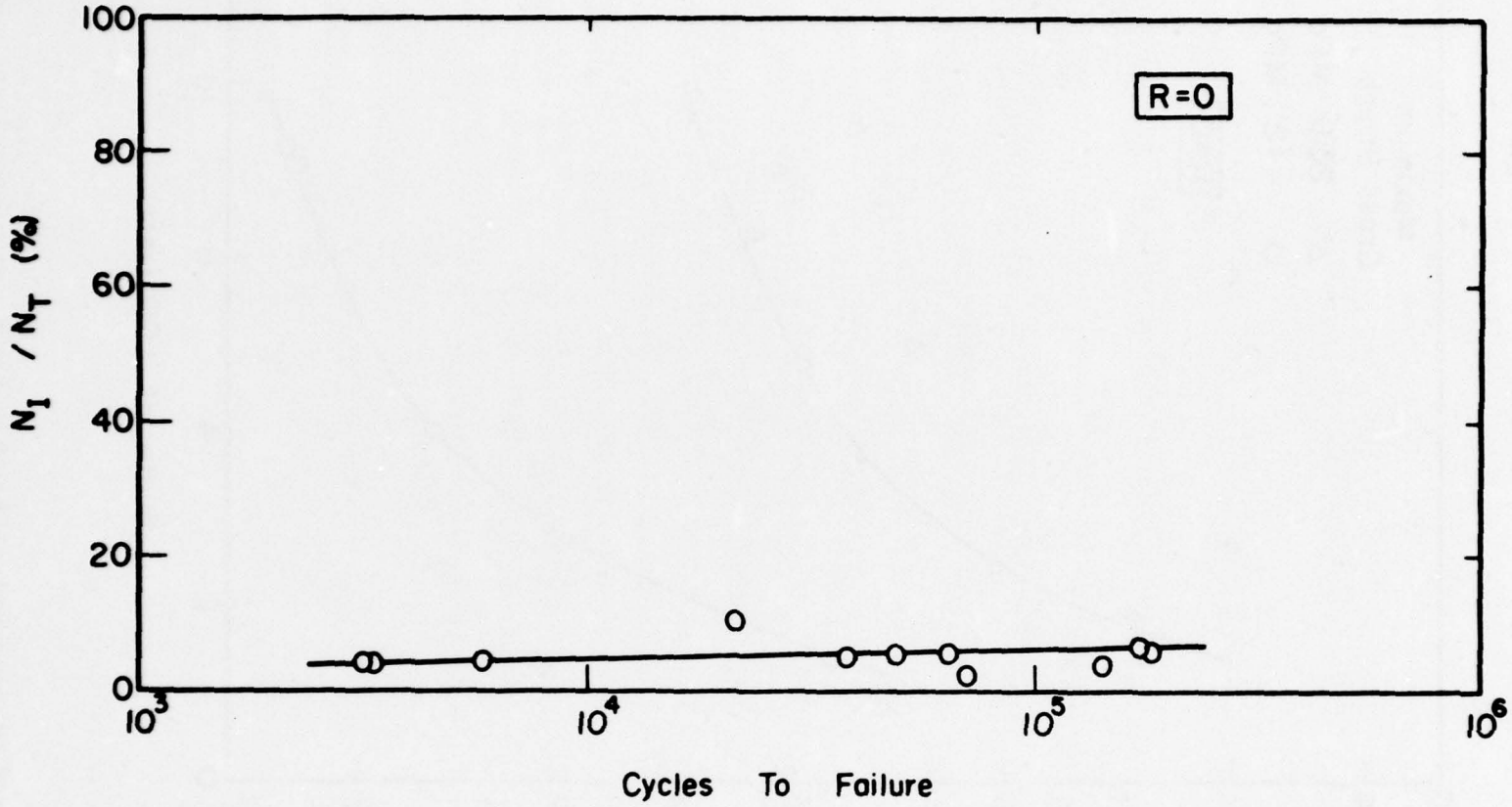

Figure 12. Percentage of life devoted to fatigue crack initiation as a function of total life.

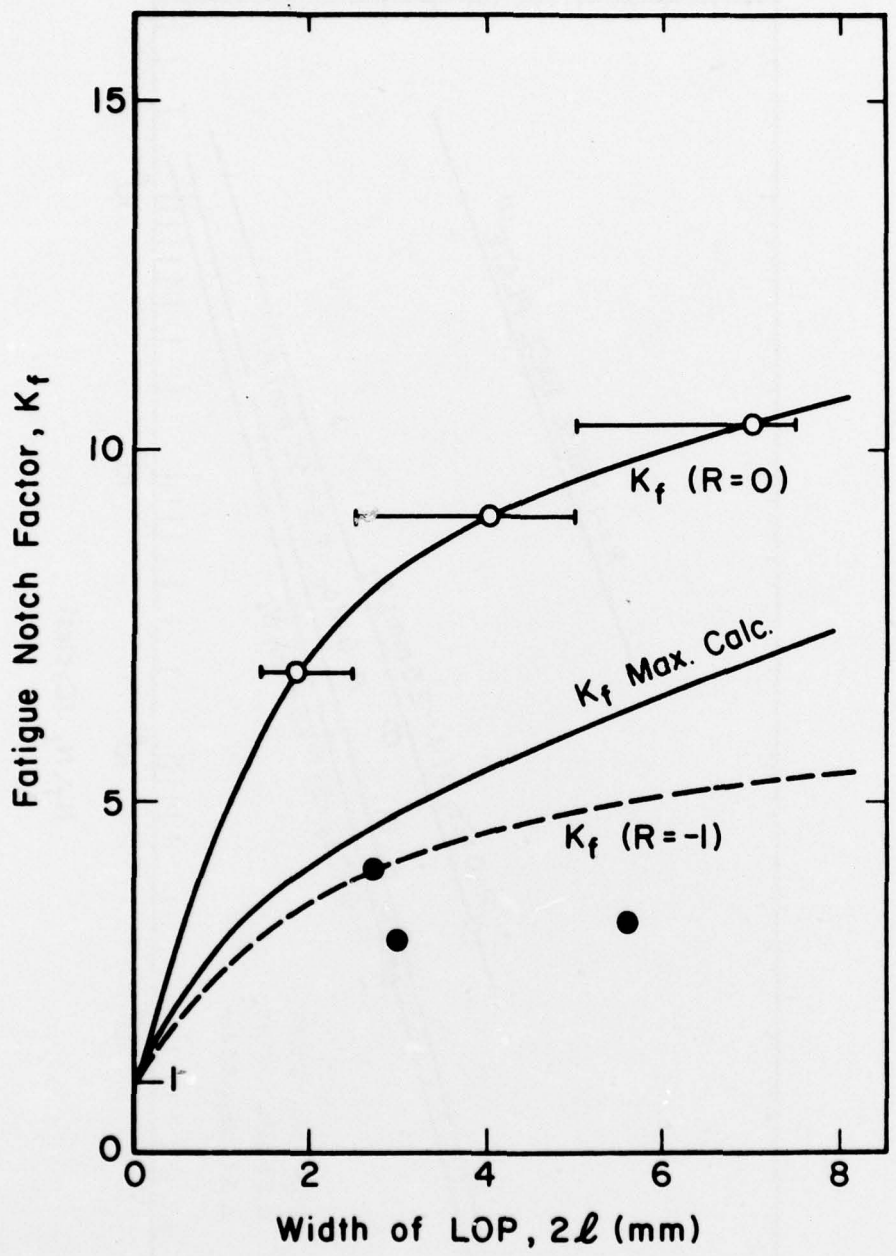

Figure 13. Comparison of values of fatigue notch factor (K_f) derived from R = 0 and R = -1 long life fatigue tests with calculated values assuming $K_{f\,max}$ conditions.

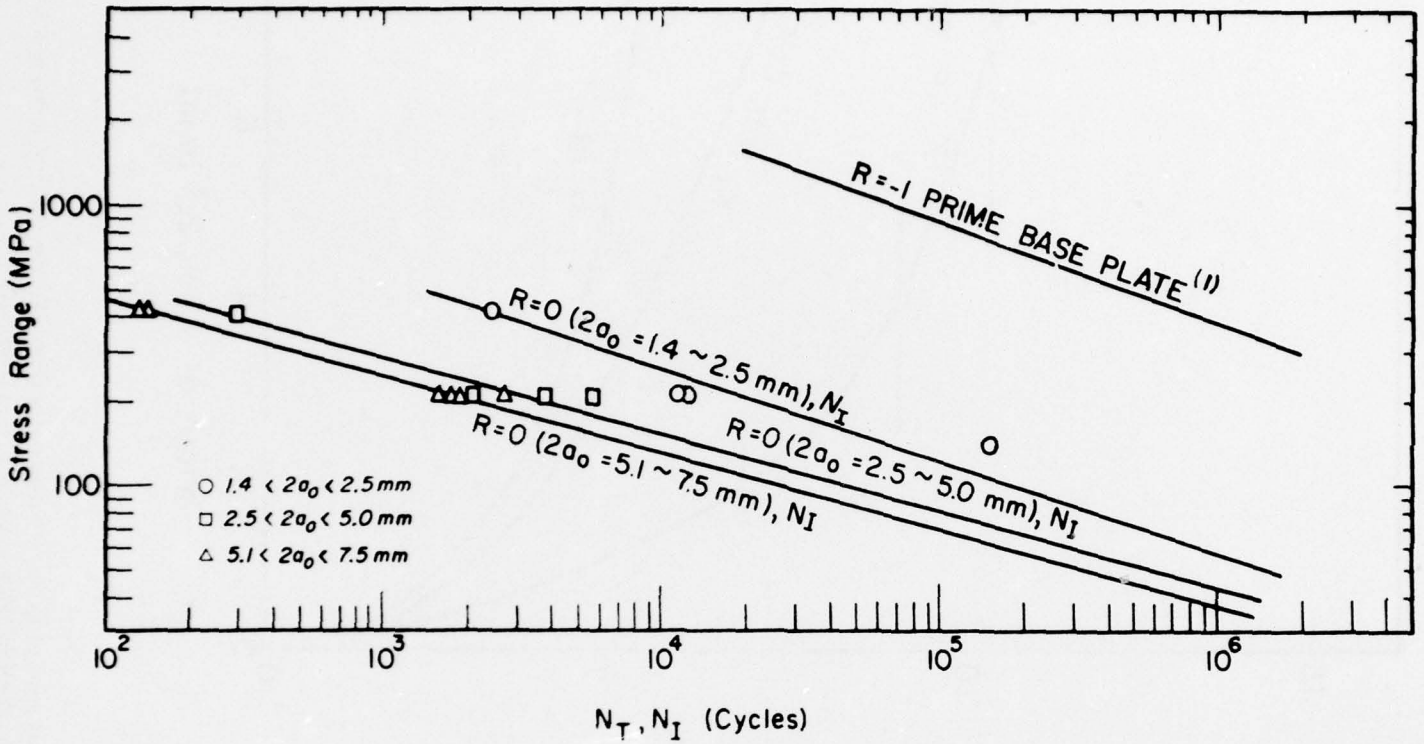

Figure 14. Stress versus cycles to failure for prime base plates (R = -1) and cycles to initiation for LN series containing LOP (R = 0).

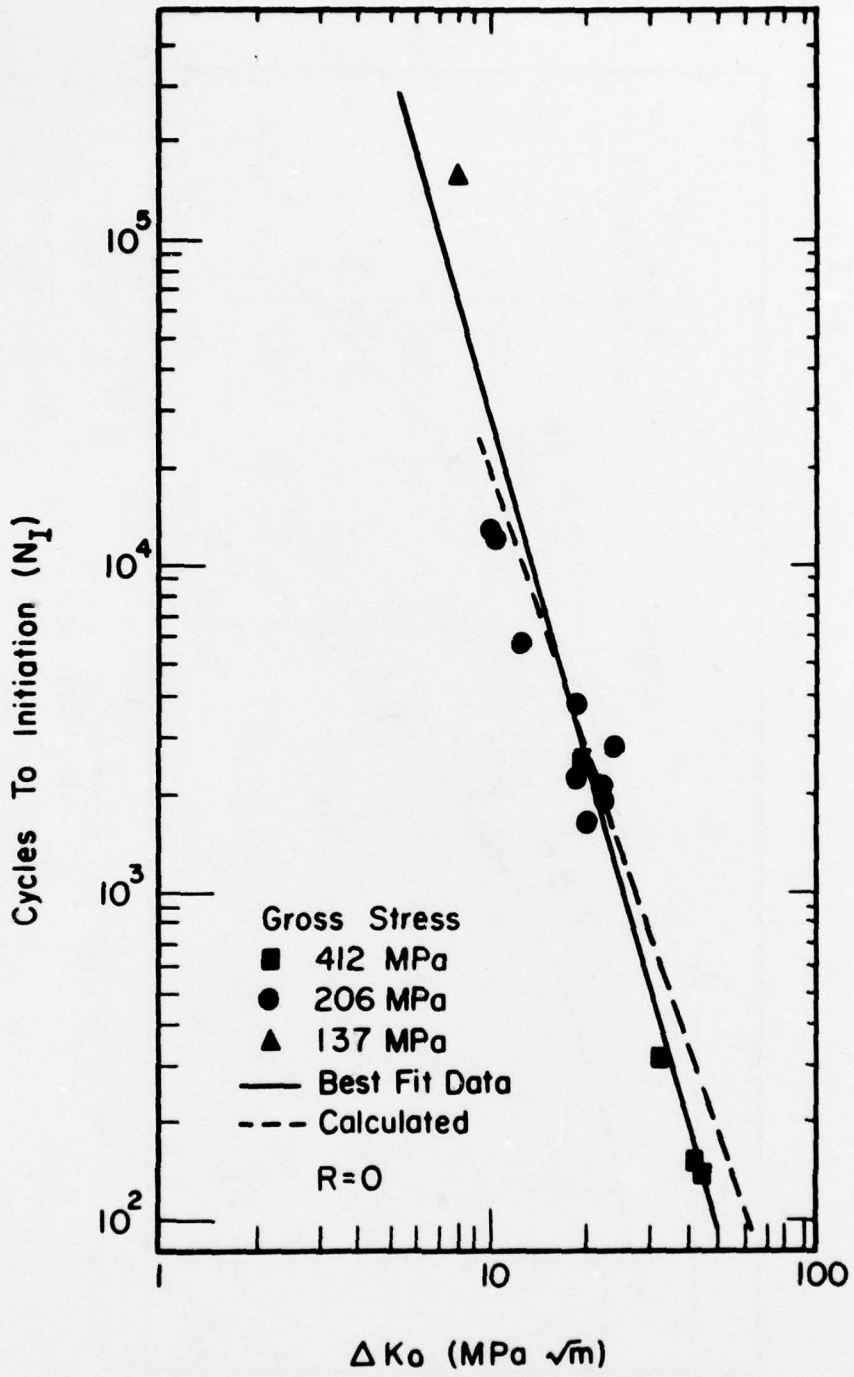

Figure 15. Relationship between initial range in stress intensity factor ($\Delta K_O = S\sqrt{\pi a_O}$) and fatigue crack initiation life.

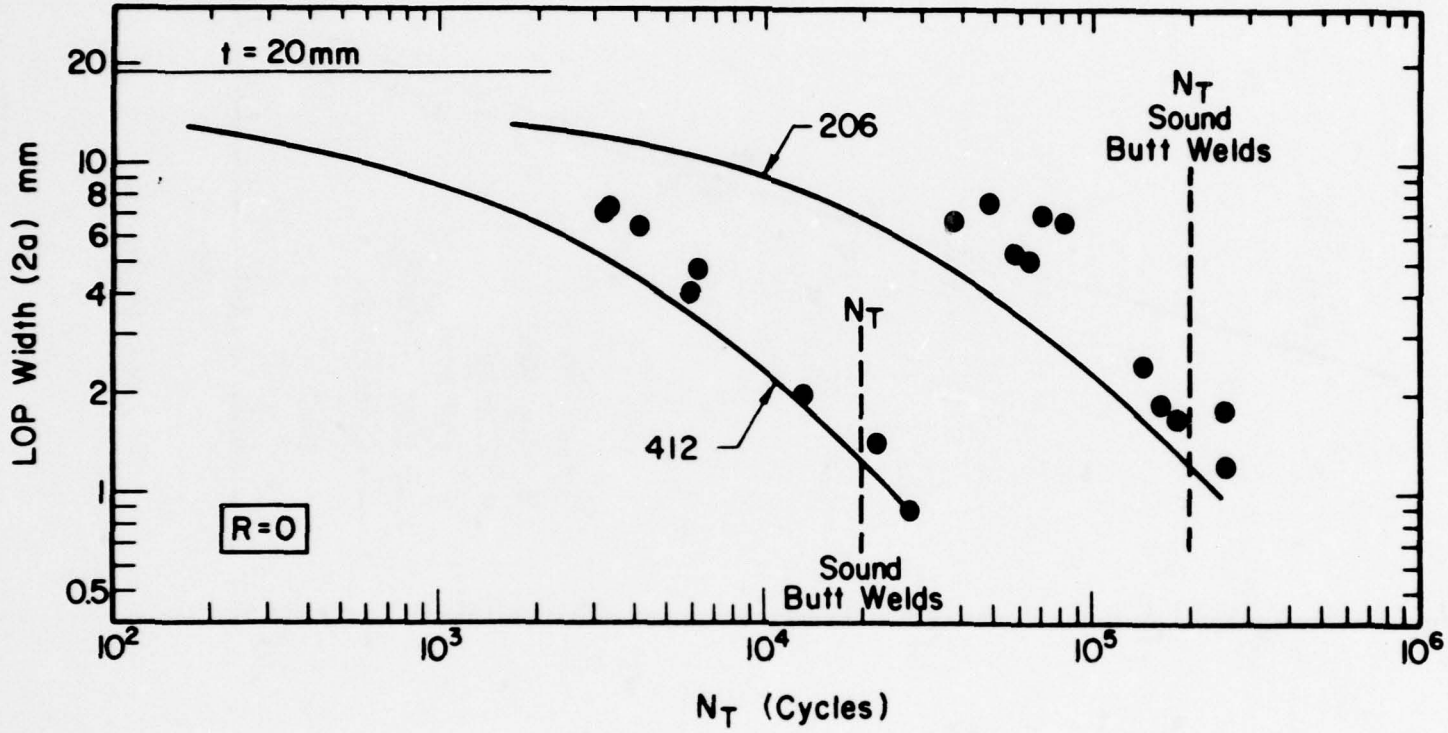

Figure 16. Initial LOP width ($2a_o$) versus total life ($N_T \simeq Np$). Solid curves were calculated using Eq 14 ($C = 1.48 \times 10^{-10}$ (MPa$\sqrt{m}$), $n = 3.32$, $K_c = 241$ MPa$\sqrt{m}$). Vertical dashed lines indicate lower confidence limits for sound butt welds with reinforcement intact.

APPENDIX A

TEST RESULTS FOR SPECIMENS CONTAINING CLUSTERED POROSITY

Supplied specimens were run to failure under a stress range of 358 MPa (R = 0).

Specimen No.	N_T (Cycles)	Failure Location
1	88,950	toe
2	32,350	large complex pore
3	33,000	clustered porosity
4	58,410	toe (and porosity)
5	32,540	LOF (and porosity)
6	30,420	large aligned pore clusters

APPENDIX B

DERIVATION OF EXPRESSION FOR FATIGUE CRACK INITIATION LIFE

A relationship between the notch root stresses and strains (σ, ϵ) and the remotely applied stresses and strains (S, e) has been developed by Neuber:

$$K_t = (K_\sigma K_\epsilon)^{1/2} \qquad \text{[Eq B1]}$$

where:

$$K_\sigma = \frac{\Delta\sigma}{\Delta S}; \quad K_\epsilon = \frac{\Delta\epsilon}{\Delta e}$$

Equation B1 can be written as

$$K_t(\Delta S \Delta e)^{1/2} = (\Delta\sigma\Delta\epsilon)^{1/2} \qquad \text{[Eq B2]}$$

If the body remains elastic remote from the notch, $\Delta e = E\Delta S$, and

$$K_t\left(\frac{\Delta S^2}{E}\right)^{1/2} = (\Delta\sigma\Delta\epsilon)^{1/2} \qquad \text{[Eq B3]}$$

rearranging

$$K_t\Delta S = (E\Delta\sigma\Delta\epsilon)^{1/2} \qquad \text{[Eq B4]}$$

Topper has shown that for fatigue applications, K_t should be replaced by K_f, the fatigue strength reduction factor.

$$K_f S = (E\Delta\sigma\Delta\epsilon)^{1/2} \qquad \text{[Eq B5]}$$

The fatigue strength reduction factor may be determined by long-life fatigue tests as the ratio of the unnotched fatigue strength to the notched fatigue strength at a given life or K_f can be estimated from the empirical relationship suggested by Peterson:

$$K_f = 1 + \frac{K_t - 1}{1 + \frac{A}{r}} \qquad \text{[Eq B6]}$$

where

K_t = elastic stress concentration factor
r = notch root radius
A = parameter characteristic of the material.

The parameter A may be estimated by the relationship:

$$A \approx 3.397 \times 10^{-3}\left(\frac{2068}{S_u}\right)^{1.8} \qquad \text{[Eq B7]}$$

For LOP defects the elastic stress concentration factor K_t may be approximated by the stress concentration of an elliptical flaw of half-width (a) and tip radius (r):

$$K_t = 1 + 2\left(\frac{a}{r}\right)^{1/2} \qquad \text{[Eq B8]}$$

Substitution of Eq B8 in Peterson's equation (Eq B6) leads to:

$$K_f = 1 + \frac{2\left(\frac{a}{r}\right)^{1/2}}{1 + \frac{A}{r}} \qquad \text{[Eq B9]}$$

Equation B9 attains a maximum value of K_f ($K_{f\,max}$) when r = A. This maximum value of K_f ($K_{f\,max}$) is the highest possible value and is presumed to occur at some location along the tip of the LOP defect, which is, of course, an irregularly shaped defect.

$$K_{f\,max} = 1 + \left(\frac{a}{A}\right)^{1/2} \qquad \text{[Eq B10]}$$

Using Eq B10, the right-hand side of Eq B5 can be expressed as:

$$K_f \Delta S = \Delta S \left(1 + \left(\frac{a}{A}\right)^{1/2}\right) \approx \Delta S \left(\frac{a}{A}\right)^{1/2} \qquad \text{[Eq B11]}$$

Now the quantity $\Delta S\sqrt{c}$ may be thought of as related to the initial value of the stress intensity factor ΔK_o associated with the LOP defect.

$$\Delta K_o \approx \Delta S\sqrt{\pi a_o} \qquad \text{so,} \qquad \text{[Eq B12]}$$

$$\frac{\Delta K}{\sqrt{\pi}} = \Delta S\sqrt{a_o} \qquad \text{[Eq B13]}$$

where a_o is the half-width of the LOP defect.

$$K_f \Delta S = \frac{K_o}{\sqrt{\pi A}} \qquad \text{[Eq B14]}$$

Assuming that the elastic strains are small relative to the plastic strains, i.e.,

$$\Delta \epsilon_T = \Delta \epsilon_e + \Delta \epsilon_p \approx \Delta \epsilon_p \qquad \text{[Eq B15]}$$

the right-hand side of Eq B5 can be expanded using stress amplitude-life and strain amplitude-life relationships:

$$\frac{\Delta \sigma}{2} = \sigma_f' (2N_I)^b \qquad \text{[Eq B16]}$$

$$\frac{\Delta \epsilon_I}{2} \approx \frac{\Delta \epsilon_p}{2} = \epsilon_f' (2N_I)^c \qquad \text{[Eq B17]}$$

where

σ_f' = fatigue strength coefficient

ϵ_f' = fatigue ductility coefficient

b = fatigue strength exponent

c = fatigue ductility exponent

N_I = fatigue crack initiation life.

Substituting Eqs B14, B16, and B17 into Eq B5 leads to

$$\frac{K_o}{\sqrt{\pi A}} = (4E\sigma_f'\epsilon_f')^{1/2} (2N_I)^{\frac{b+c}{2}} \qquad \text{[Eq B18]}$$

which can be solved for the fatigue crack initiation life, N_I:

$$N_I = \frac{1}{2}\left[\frac{\sqrt{4\pi A E \sigma_f' \epsilon_f'}}{K_o}\right]^{\frac{2}{|b| + |c|}} \qquad \text{[Eq B19]}$$

REFERENCES

Bucci, R. J., et al., *Fatigue Crack Propagation Growth Rates Under a Wide Variation of ΔK for an ASTM A-517 Grade F (T - 1) Steel,* ASTM STP 513 (American Society for Testing and Materials, September 1972).

Mattos, R. J., *Estimation of the Fatigue Crack Initiation Life in Welds Using Low Cycle Fatigue Concept*, Ph.D. Thesis (University of Illinois at Urbana-Champaign, 1975).

Munse, W. H., et al., *Fatigue Data Bank and Data Analysis Investigation*, Structural Research Series No. 405 (University of Illinois at Urbana-Champaign, June 1973).

Neuber, H., "Theory of Stress Concentration for Shear Strained Prismatical Bodies with Arbitrary Non-Linear Stress-Strain Laws," *Journal of Applied Mechanics* (December 1961), p 544.

Paris, P. C., et al., "A Critical Analysis of Crack Propagation Laws," *Trans. ASME (D)*, Vol 85, No. 4 (1963).

Peterson, R. E., "Fatigue of Metals III—Engineering and Design Aspects," *Materials Research and Standards*, Vol 6, No. 6 (February 1963), p 313.

CERL DISTRIBUTION

Director of Facilities Engineering
APO NY 09827

DARCOM STIT-EUR
APO New York 09710

West Point, NY 10996
ATTN: Dept of Mechanics
ATTN: Library

Chief of Engineers
ATTN: DAEN-ASI-L (2)
ATTN: DAEN-MCE-D
ATTN: DAEN-MCZ-S
ATTN: DAEN-RDL
ATTN: DAEN-PMS (6)
for forwarding to
National Defense Headquarters
Director General of Construction
Ottawa, Ontario K1A0K2
Canada

Canadian Forces Liaison Officer (4)
U.S. Army Mobility Equipment
Research and Development Command
Ft Belvoir, VA 22060

Airports and Const. Services Dir.
Technical Information Reference
Centre
K40L, Transport Canada Building
Place de Ville, Ottawa, Ontario
Canada, K1A0N8

Ft Belvoir, VA 22060
ATTN: Kingman Bldg, Library

Ft Monroe, VA 23651
ATTN: ATEN

Ft McPherson, GA 30330
ATTN: AFEN-FED

USA-WES
ATTN: Library

6th USA
ATTN: AFKC-LG-E

US Army Science & Technology Center
- Far East Office

US Army Engineer District
Buffalo
ATTN: Library
Pittsburgh
ATTN: Library
Philadelphia
ATTN: Library
ATTN: Chief, NAPEN-D
Baltimore
ATTN: Chief, Engr Div
Norfolk
ATTN: Chief, NAOEN-D
Wilmington
ATTN: Chief, SAWEN-D
Charleston
ATTN: Chief, Engr Div
Savannah
ATTN: Library
ATTN: Chief, SASAS-L
Jacksonville
ATTN: Library
ATTN: Const. Div
Mobile
ATTN: Chief, SAMEN-C
ATTN: Chief, SAMEN-D
Nashville
ATTN: Library
Memphis
ATTN: Chief, LMMED-DM
Vicksburg
ATTN: Chief, Engr Div
Louisville
ATTN: Chief, Engr Div
St Paul
ATTN: Chief, ED-D
St Louis
ATTN: Library
Kansas City
ATTN: Library (2)
Omaha
ATTN: Chief, Engr Div

US Army Engineer District
New Orleans
ATTN: Library
ATTN: Chief, LMNED-DG
Little Rock
ATTN: Chief, Engr Div
Tulsa
ATTN: Library
Albuquerque
ATTN: Library
San Francisco
ATTN: Chief, Engr Div
Sacramento
ATTN: Chief, SPKED-D
Japan
ATTN: Library
Portland
ATTN: Chief, DB-6
Seattle
ATTN: Chief, NPSCO
Walla Walla
ATTN: Library
ATTN: Chief, Engr Div
Alaska
ATTN: Library
ATTN: NPADE-R

US Army Engineer Division
Europe
ATTN: Technical Library
New England
ATTN: Library
ATTN: Chief, NEDED-T
North Atlantic
ATTN: Chief, NADEN-T
South Atlantic
ATTN: Chief, SADEN-TS
ATTN: Library
Huntsville
ATTN: Library (2)
ATTN: Chief, HNDED-CS
ATTN: Chief, HNDED-SR
Lower Mississippi Valley
ATTN: Library
Ohio River
ATTN: Library
ATTN: Chief, Engr Div
North Central
ATTN: Library
Missouri River
ATTN: Library (2)
Southwestern
ATTN: Library
ATTN: Chief, SWDED-TM
Pacific Ocean
ATTN: Chief, Engr Div
North Pacific
ATTN: Chief, Engr Div

AF Civil Engr Center/XRL
Tyndall AFB, FL 32401

Naval Air Systems Command
ATTN: Library
WASH DC 20360

Naval Facilities Engr Command
ATTN: Code 04
Alexandria, VA 22332

Port Hueneme, CA 93043
ATTN: Library (Code L08A)

Washington, DC
ATTN: Transportation Research Board
ATTN: Library of Congress (2)
ATTN: Dept of Transporation Library

Defense Documentation Center (12)

Engineering Societies Library
New York, NY 10017